ACS APPLIED MATERIALS & INTERFACES

Research Article

www.acsami.org

Encapsulated Silicene: A Robust Large-Gap Topological Insulator

Liangzhi Kou,*[,†] Yandong Ma,[‡] Binghai Yan,[§] Xin Tan,[†] Changfeng Chen,[∥] and Sean C. Smith*[,†]

[†]Integrated Materials Design Centre (IMDC), School of Chemical Engineering, University of New South Wales, Sydney, NSW 2052, Australia

[‡]Engineering and Science, Jacobs University Bremen, Campus Ring 1, 28759 Bremen, Germany

[§]Max Planck Institute for Chemical Physics of Solids, Noethnitzer Str. 40, 01187 Dresden, Germany

[∥]Department of Physics and Astronomy and High Pressure Science and Engineering Center, University of Nevada, Las Vegas, Nevada 89154, United States

Supporting Information

ABSTRACT: The quantum spin Hall (QSH) effect predicted in silicene has raised exciting prospects of new device applications compatible with current microelectronic technology. Efforts to explore this novel phenomenon, however, have been impeded by fundamental challenges imposed by silicene's small topologically nontrivial band gap and fragile electronic properties susceptible to environmental degradation effects. Here we propose a strategy to circumvent these challenges by encapsulating silicene between transition-metal dichalcogenides (TMDCs) layers. First-principles calculations show that such encapsulated silicene exhibit a two-orders-of-magnitude enhancement in its nontrivial band gap, which is driven by the strong spin−orbit coupling effect in TMDCs via the proximity effect. Moreover, the cladding TMDCs layers also shield silicene from environmental gases that are detrimental to the QSH state in free-standing silicene. The encapsulated silicene represents a novel two-dimensional topological insulator with a robust nontrivial band gap suitable for room-temperature applications, which has significant implications for innovative QSH device design and fabrication.

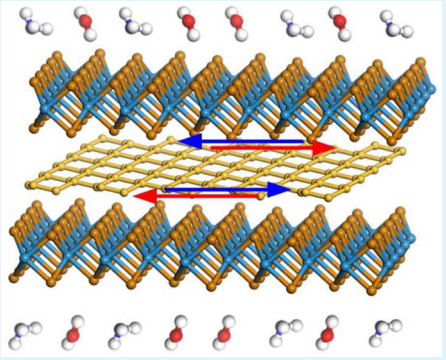

KEYWORDS: *silicene, encapsulation, topological insulator, large gap, proximity effect, first-principles calculations*

INTRODUCTION

Topological insulators (TIs) have emerged in recent years as a new class of materials that exhibits a novel quantum state of matter. The quantum spin Hall (QSH) state in TIs provides new possibilities for low-dissipation spintronic devices due to the absence of backscattering and possible superconductivity.[1−4] Silicene, a graphene analogue of silicon, has been synthesized[5,6] and predicted[7] to possess a QSH state, raising the exciting prospects of new device applications of such single-layer silicon materials that are compatible with current microelectronic technologies. The recent report[8] of successful fabrication of field-effect transistors (FETs) based on silicene introduces possibilities of solving the major problem of heating in conventional silicon-based FETs, which represents over 90% of device energy consumption. There are, however, fundamental challenges that must be resolved before practical device applications of silicene can be realized. Prominent among these challenges are the extremely small intrinsic nontrivial band gap (1.5 meV) and highly sensitive nature of silicene to the environmental gases that severely degrade its electronic properties.[9,10]

A novel feature of TIs is their ability to host conducting states on edges or surfaces while behaving as an insulator in the interior.[11,12] These metallic surface or edge states comprise pairs of states that have opposite spins and propagate in opposite directions, thus forming pure dissipationless spin currents. Protected by the time-reversal symmetry and nontrivial topological order, these states are robust against backscattering and nonmagnetic impurities. These properties could make possible spintronic devices and practical quantum computers far more powerful than those supported by today's technologies. So far, a large number of three-dimensional (3D) TIs have been theoretically predicted and some experimentally confirmed, such as chalcogenides (e.g., HgTe),[13] the Bi_2Se_3 family,[4] and oxides ($BaBiO_3$).[14] Meanwhile, 2D TIs have been attracting increasing attention due to their lower dimensionality that is easily compatible with device configurations and offers more functionalities. Subsequently, a number of 2D TI compounds have been identified, such as germanene,[7] $ZeTe_5$ monolayers,[15] and chemically modified stanene and bismuth bilayer.[16,17] Although some 2D TIs are predicted to possess large nontrivial band gaps,[18] these materials are not compatible with current silicon-based computer technologies.

Despite the experimental reports on silicene synthesis on the Ag (111) surface,[5,6] free-standing silicene has not yet been fabricated and the experimental confirmation of its topological

Received: June 9, 2015
Accepted: August 20, 2015
Published: August 20, 2015

DOI: 10.1021/acsami.5b05063
ACS Appl. Mater. Interfaces 2015, 7, 19226−19233

phase still remains elusive. This situation is attributed to two main reasons: (i) the very-small nontrivial band gap of 1.5 meV limits its observation, which requires a working temperature down to about 18 K since it is vulnerable to thermal fluctuations;[7] (ii) silicene possesses a chemically very active surface, which is sensitive to the enviorment.[9,10,19] Gas molecules like NO, NO_2, NH_3, SO, SO_2, CO, and CO_2 tend to be adsorbed on the silicene surface, which can significantly change the electronic properties and turn it into a topologically trivial semiconductor. Particularly, O_2 in air can remarkably degrade the intrinsic Dirac cone and its topological features.[19] Two urgent questions therefore arise in regard to silicene usage in nanodevice applications: (i) how to protect silicene from environmental degradation, and (ii) how to significantly increase the nontrivial band gap into a practical application range.

Encapsulation technology, which has been used in Flip-Chip,[20] is one of the possibilities for resolution of the silicene predicament. Recent first-principles calculations showed that the electronic properties of silicene can be tuned by the composition of MoX_2 and GaX (X = S, Se, Te).[21,22] Using suitable cladding layers with strong spin−orbit coupling (SOC) could simultaneously enhance the intrinsic SOC and nontrivial band gap of silicene and prevent the environmental degradation of its electronic properties. The technical feasibility of such an approach has been demonstrated in recently fabricated silicene FETs where silicene is encapsulated between protective cladding layers during the transfer and device fabrication process.[8] This strategy also has been used in other systems. For example, a hybrid structure of a graphene layer interfaced with a Bi_2Se_3 or BiTeX (X = Cl, Br, and I) has been proposed to produce a 2D TI;[23,24] and proximity effects have been observed in a MoS_2 layer interfaced with NbS_2, resulting in 1D topological superconductivity that offers a platform for realizing Majorana Fermions for quantum computation applications.[25,26]

In this work we show by extensive first-principles calculations that a hybrid QW structure consisting of a monolayer silicene encapsulated by a TMDCs MTe_2 (M = Mo or W) layer on each side forms a novel 2D TI with a drastically enhanced nontrivial band gap that is 2 orders of magnitude higher than its value in free-standing silicene. This striking behavior is driven by the strong SOC in the MTe_2 layers via the proximity effect, which is sensitive to the interlayer coupling and highly effective in generating QSH states with a large nontrivial band gap in silicene in the QW architecture. Moreover, the cladding MTe_2 layers also protect silicene from the degradation effects by the environmental gases, which, if not prevented, would destroy the QSH states. The topological nature of the QW structure is explicitly demonstrated by the presence of metallic edge states that are characteristic of the QSH states in 2D TIs. We further show that the QSH states in encapsulated silicene are robust against stacking misalignments that will likely exist in synthesized QW structures due to the lattice mismatch between the silicene layer and the cladding MTe_2 layers. The present work offers a new design concept for a novel class of 2D TIs that can operate in room temperature environments, and our current results are expected to stimulate considerable interest and further exploration that could lead to innovative nanoscale device applications with the new TMDCs encapsulated silicene QW structure as a central component.

RESULTS

Structural and Electronic Properties of Encapsulated Silicene. The MX_2 (M = Mo, W; X = S, Se, Te) layered materials comprise X-M-X trilayers coupled by the van der Waals (vdW) interaction. This quasi-2D structural feature facilitates the fabrication of such layered TMDCs in ultrathin films by micromechanical cleavage and exfoliation methods.[27,28] The absence of inversion symmetry in TMDCs introduces a giant spin splitting of 148−456 meV at the K points of the 2D Brillouin zone, leading to the coupled spin and valley physics in the monolayers.[29,30] Among the dichalcogenides, $MoTe_2$ and WTe_2 are both semiconductors with strong spin splitting,[31,32] making them good candidates for influencing silicene via proximity effects. Here we first use hexagonal 2H-WTe_2 as the cladding material. The fully relaxed lattice constants of free-standing silicene (low-buckled) and 2H-WTe_2 are 3.86 and 3.57 Å, respectively, which are consistent with previous reports.[7,32] We constructed the QW model by sandwiching the unit cell of silicene between two WTe_2 layers, and then fully relaxed the lattice constant and atom positions, obtaining a global lattice constant of 3.65 Å, which is closer to the value for WTe_2 that is stiffer than silicene.[33,34]

Before exploring the hybrid QW structure, we first check the effect of strain on each single component, namely, monolayer silicene and trilayer 2H-WTe_2. Figure 1 shows the calculated

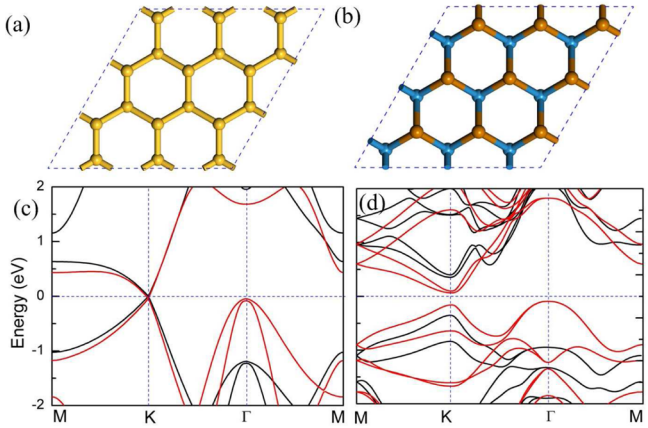

Figure 1. Lattice and electronic band structure of free-standing silicene and WTe_2. The lattice model and electronic band structure of strain-free (black lines) and strained (red lines) silicene are shown in (a) and (c), respectively. The corresponding results for 2H-WTe_2 are shown in (b) and (d). The yellow balls represent Si atoms, while the blue and brown balls are Te and W atoms, respectively.

electronic band structure of each single component at equilibrium compared to the results at the global lattice constant of 3.65 Å for the QW structure. It is seen that a Dirac cone exists in the free-standing silicene with a nontrivial band gap of 1.5 meV, which is consistent with the previously reported result.[7] At the QW lattice constant of 3.65 Å, this nontrivial band gap increases to 2.5 meV with the Dirac cone at the K point well preserved. While the valence band maximum at the Γ point is upshifted by the intralayer strain, the main characteristics of silicene (Dirac cone and Fermi velocity) remain essentially unchanged. Trilayer 2H-WTe_2 exhibits a direct band gap of 0.71 eV at the K points, which is slightly smaller than previously reported values,[31,32] caused by the SOC-induced band splitting. As shown in Figure 1d, there is a

DOI: 10.1021/acsami.5b05063
ACS Appl. Mater. Interfaces 2015, 7, 19226−19233

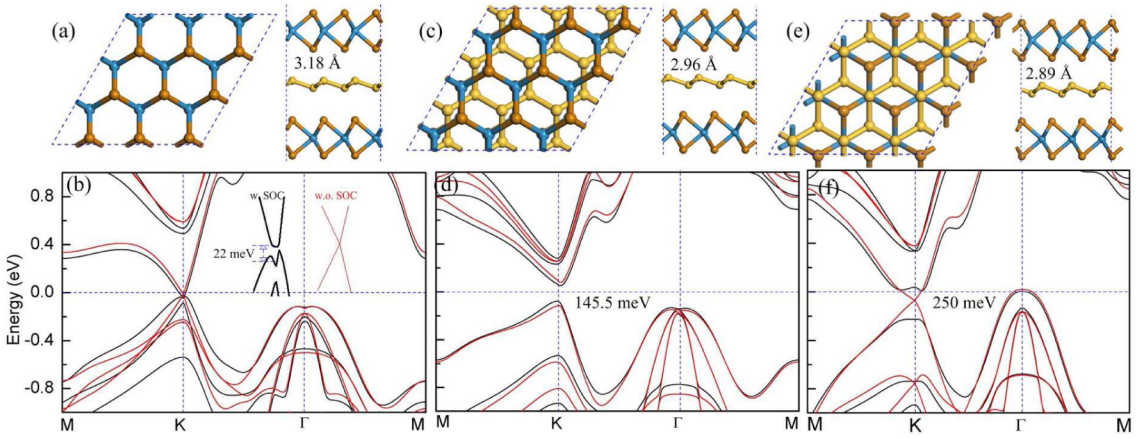

Figure 2. Lattice and electronic band structures of differently stacked QWs. The AA, MA, and AB stacking patterns between silicene and WTe_2 are displayed in (a), (c), and (e), respectively, while the corresponding electronic band structures are presented in (b), (d), and (f), where black (red) lines are those with (without) the SOC effect.

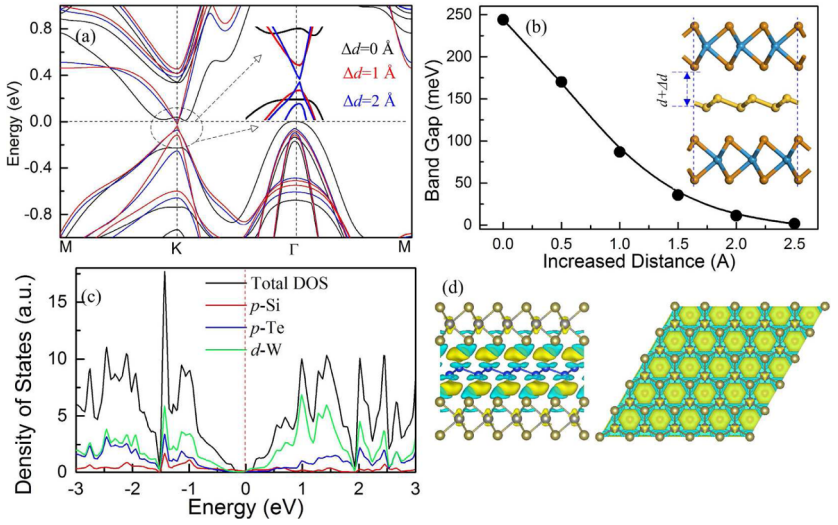

Figure 3. Analysis of the band gap enhancement induced by the proximity effect. (a) Variation of the band structure of the AB stacked QW at different interlayer distances; the black, blue, and red lines are for the cases with the distance increase of 0, 1, and 2 Å, respectively. (b) The band gap as a function of the interlayer distance increase. (c) Partial density of states that show strong hybridizations around the Fermi level. (d) Charge transfer between the silicene and cladding layers.

band splitting of 487 meV for the valence band states near the Fermi level, close to the predicted value in WSe_2.[29] At the QW lattice constant of 3.65 Å, the band gap is reduced by strain to 0.23 eV; but the semiconducting nature and the giant SOC induced band splitting remain unchanged. These results show that the basic physics of free-standing silicene and trilayer MTe_2 remain the same in the QW structure.

We now examine the hybridization and proximity effect in the QW structure. Three typical stacking patterns at the interface between silicene and WTe_2 are shown in Figure 2a,c,e: (i) the AA stacking, where each Si atom is on top of either a W or Te atom; (ii) the MA stacking, where the silicene layer is shifted (by half of a unit-cell length) with respect to the WTe_2 layers and the Si atoms are misaligned (thus termed MA) relative to the W and Te atoms; and (iii) the AB stacking, where each Si atom is either on top of a W atom or a hexagonal center. There are other ways to construct a QW in MA stacking; but, as will be shown below, the essential physics will remain the same. In the QW architecture, the silicene layer is sandwiched between two WTe_2 layers. This structural arrangement protects the silicene layer from environmental degradation effects (see below for details), and it also maintains the structural inversion symmetry, thus removing the Rashba (dipole) effect. After a full structural relaxation, the interlayer distances (the nearest distance between the Si and Te atoms along the vertical direction) are calculated to be 3.18, 2.96, and 2.89 Å for the three stacking patterns, respectively, and these large distances indicate that the interlayer interaction is dominated by vdW forces. To determine the structural stability, we have calculated the formation energy $E_f = E_{WTe2} + E_{silicene} - E_{tot}$, where E_{tot} is the total energy of the hybrid QW structure, E_{WTe2} is the energy of a double-layer WTe_2 with the interlayer distance taking the value of the hybrid structure, and $E_{silicene}$ is the energy of free-standing silicene. The calculated results show that the AB stacking configuration has the largest formation energy, 0.86 eV/unit-cell, and the AA stacking structure has the lowest value, 0.55 eV/unit-cell, while the result for the MA stacking, 0.67 eV/unit-cell, lies in between.

The QW structures with different stacking patterns show distinct electronic properties. For the AA (Figure 2a) and AB

DOI: 10.1021/acsami.5b05063
ACS Appl. Mater. Interfaces 2015, 7, 19226−19233

(Figure 2e) stacking configuration where the sublattice symmetry is maintained in the absence of the SOC, a well-defined Dirac cone can be observed at the K point of the Brillouin zone in each case (Figure 2b and f), which resembles that seen in free-standing silicene. In contrast, the MA stacking configuration (Figure 2c) shows a finite band gap opening at the K point (Figure 2d) caused by the lattice symmetry breaking in the MA stacking (a similar gap opening will occur in all QWs with an MA stacking, regardless of the details of the relative atomic position misalignment between different layers). When the SOC is switched on, all the band structures undergo dramatic changes, especially the band states near the Fermi level at the K point. The band gap of the AA stacking configuration increases to 22 meV at the K point, which is an order of magnitude larger than the value for free-standing silicene. The most significant SOC-induced band gap opening occurs in the AB stacking configuration, where a band gap reaches 250 meV around the K point. Meanwhile, the band gap of the MA stacking configuration is 145.5 meV. These results show a clear correlation between the sizes of the nontrivial band gap with the stacking patterns that have different interlayer distances. This correlation suggests that the strong SOC effects in the WTe_2 layers play a prominent role in influencing the electronic band structure of the silicene layer via the proximity effect.

For a quantitative understanding of the SOC-enhanced band gap in encapsulated silicene via the proximity effect, we performed systematic electronic structure calculations on a series of QW structures with a controlled variation of the interlayer distance. The calculated results show the same trend in the interlayer-distance dependence of the nontrivial band gap for all three stacking patterns. Here we present a detailed analysis for the case of the AB stacking (see Figure S1 in Supporting Information for the results of the AB and MA stacking cases). Results in Figure 3 show that at an interlayer distance of 5.39 Å, i.e., an increase of Δd = 2.5 Å from the equilibrium value of 2.89 Å for the AB stacking, the band gap at the K point is 1.5 meV, which is the same value for free-standing silicene. As the interlayer distance is reduced, which can be achieved by applying an external uniaxial stress perpendicular to the WTe_2 sheet,[35] the valence band and conduction band move apart around the Fermi level at the K point, resulting in a steady increase of the band gap. At the equilibrium interlayer distance of 2.89 Å the band gap rises by 2 orders of magnitude to 250 meV. These results indicate that the band gap enhancement is driven by an interlayer-distance-sensitive proximity effect, which is similar to the previously reported case of graphene on WSe_2.[36] The underlying mechanism here is the orbital hybridization between silicene and WTe_2 through charge transfer, which also has been seen in heavy-metal enhanced spin−orbit effects on graphene.[37] A partial density of states (PDOS) analysis (Figure 3c) shows that the Si *p*-orbital has a strong overlap with those from W 5d-orbital and Te 5p-orbital in the energy range −2 to 2 eV, indicating substantial hybridization between the silicene and WTe_2 layers. This is further supported by a charge transfer analysis (Figure 3d), where the charge transfer is defined as $\rho(r) = \rho_{tot}(r) - \rho_{Silicene}(r) - \rho_{WTe2}(r)$. Adjacent Te atoms are electron depleted while silicene is gaining electrons by 0.01 e/Si from WTe_2 according to a Bader charge analysis.

Explicit Demonstration of the TI Phase and Edge States in Encapsulated Silicene. To confirm the band topology of encapsulated silicene, we have analyzed its Z_2 topological invariant (ν). The calculations lead to the same conclusion for all three stacking cases. Below we will focus on the AB stacking in our discussions. According to the Z_2 classification, ν = 1 characterizes a topologically nontrivial phase and ν = 0 means a topologically trivial phase.[38,39] Due to the inversion symmetry in our constructed QW structure, the method developed by Fu and Kane[38,39] is applicable here; namely, the Z_2 topological invariant can be directly calculated based on the parity of the Bloch wave function for all the filled bands at all the time-reversal-invariant momenta (TRIM). Calculations were performed for four TRIM points (K_i) in the Brillouin zone, one at the Γ point and three at the M points. Accordingly, the topological indexes are established by

$$\delta(K_i) = \prod_{N}^{m=1} \xi_{2m}^{i}$$

$$(-1)^{\nu} = \prod_{4}^{i=1} \delta(K_i) = \delta(\Gamma)\delta(M)^3$$

where δ is the product of the parity eigenvalues at the TRIM points, $\xi = \pm 1$ are the parity eigenvalues, and N is the number of occupied bands. In our QW structure, there are 22 spin-degenerate bands for 44 valence electrons. Thus, we calculated the parity eigenvalues of the Bloch wave function for the 22 occupied spin-degenerate bands at all four TRIM points in the Brillouin zone. The obtained product of the parity eigenvalues at the Γ point is +1, whereas it is −1 at the M point, yielding a nontrivial topological invariant ν = 1 (see Table S1 in Supporting Information for details on parities of each valence band at all TRIM points). This result shows that the encapsulated silicene in the QW structures studied in the present work are all TIs that host the QSH effect.

A characteristic feature of 2D TIs is that they support an odd number of topologically protected gapless edge states, which connect the valence and conduction bands at certain *k*-points. For an explicit demonstration of this topological feature in encapsulated silicene, we constructed an AB-stacked armchair nanoribbon where the dangling bonds of all the edge atoms are passivated with hydrogen atoms. This nanoribbon structure contains 60 W atoms, 120 Te atoms, 60 Si atoms, and 20 H atoms (see Figure S2 in Supporting Information for the structural model). The width of the nanoribbon reaches 55 Å, which is large enough to avoid the interaction between the two edges. The calculated edge states are shown in Figure 4a, where one can clearly see the topological edge states with a single Dirac-type crossing at the Γ point. We plot in Figure 4c and d the spatial distribution of the wave function of the two sets of edge states that are localized at the opposite ends of the ribbon. To show that these helical edge states are indeed from the proximity enhanced SOC in silicene, we additionally calculated the band structure of the single silicene nanoribbon (only the middle layer) and double-layer WTe_2 ribbon (the upper and bottom layers at the fixed interlayer distance) under the same conditions, namely, the same ribbon width and atomic positons as in the heterostructure ribbon. The results are shown in Figure 4b, where one can see that the double-layer WTe_2 ribbon exhibits a large band gap at the Γ point, while the silicene ribbon also possesses a band gap of 22 meV; in other words, there are no metallic edge states in these isolated components without including the proximity effect. We therefore conclude that the metallic edge states of the

DOI: 10.1021/acsami.5b05063
ACS Appl. Mater. Interfaces 2015, 7, 19226−19233

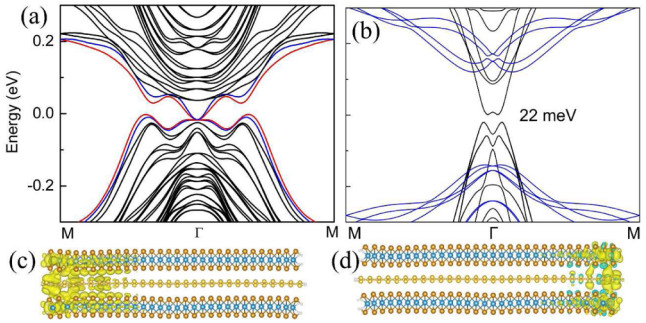

Figure 4. Helical edge states. (a) Electronic band structure of an AB-stacked armchair QW ribbon. (b) Band structures of pure silicene nanoribbon (black lines) and double-layer WTe_2 (blue lines); (c) and (d) show the spatial distribution of the wave functions of the two edge states marked with red and blue lines in (a); the isosurface is set to 5×10^{-5} e/Å^3.

heterostructure, which act as a signature of the 2D TI phase, arise from the proximity enhanced SOC in silicene.

Robustness of the TI Phase against Environmental Degradation Effects. Unlike graphene, exposed silicene is generally unstable in air. Free-standing silicene possesses a very sensitive surface, which stems from its mixed sp^2–sp^3 bonding character[40] and thus requires effective passivation or encapsulation at all stages from materials synthesis to device fabrication. However, the passivation for the surface always destroys the outstanding properties by reducing the mobility and breaking the Dirac cone.[9,10,41,42] This is one of the major reasons that TI properties of silicene have not yet been demonstrated. First-principles calculations predict that silicene will become a large-gap semiconductor and lose the topological feature when exposed to the air due to modifications by the gas molecules like NO, O_2, NH_3, and SO_2. In experiments, silicene is also easily oxidized, leading to the absence of an observed Dirac cone.[41,42] The latest development of the silicene encapsulated delamination technique, which has been successfully used to fabricate silicene-based FETs, offers a way to overcome these challenges.[8] The QW structure proposed in the present work can be regarded as an example of the silicene encapsulated technique where the cladding WTe_2 layer not only enhances the SOC effect, leading to the large nontrivial band gap as shown above, but also is able to protect the silicene from environmental degradation effects.

To showcase the effective protective role of the cladding layer, we have performed a comparative study of the electronic and band topological variation of free-standing silicene compared to encapsulated silicene.[6]

We have examined the effect of the adsorption of two typical gases, H_2O and NH_3, and the results are presented in Figure 5. For H_2O on free-standing silicene, it is a typical physisorption with an adsorption distance of 2.5 Å and an adsorption energy of 0.085 eV/unit-cell, where H_2O acts as an electron acceptor. This adsorption causes an obvious variation in the electronic band structure: a 70 meV band gap opens around the Dirac cone at the K point driven by the lattice symmetry breaking, and the band structure is insensitive to the SOC, indicating that the system is no longer in a TI state. These results demonstrate that the band topology of free-standing silicene would be vulnerable to common humidity in the air. Meanwhile, NH_3 bonds directly with silicene as an electron donor, at a much closer distance (1.91 Å) with a stronger binding energy (0.251 eV/unit-cell). This chemisorption causes more severe changes in the structural and electronic properties of silicene. The electronic property is dramatically modified as shown in Figure 5d, where the Dirac-cone feature of free-standing silicene disappears while a large gap (0.293 eV) is opened at the Γ point. The band topology is also fundamentally altered since the band structure becomes insensitive to the SOC, indicating it is not in a TI state. In stark contrast, both gas molecules are weakly chemisorbed on encapsulated silicene with a large binding distance (2.74 Å for H_2O and 3.55 Å for NH_3). They have very limited influence on the electronic properties as shown in Figure 5b and d. The Dirac cone at the K point is well preserved when the SOC is not included, and a gap of 250 meV is opened by the proximity SOC effect. A Z_2 analysis confirms that encapsulated silicene with gas molecule adsorption is a 2D

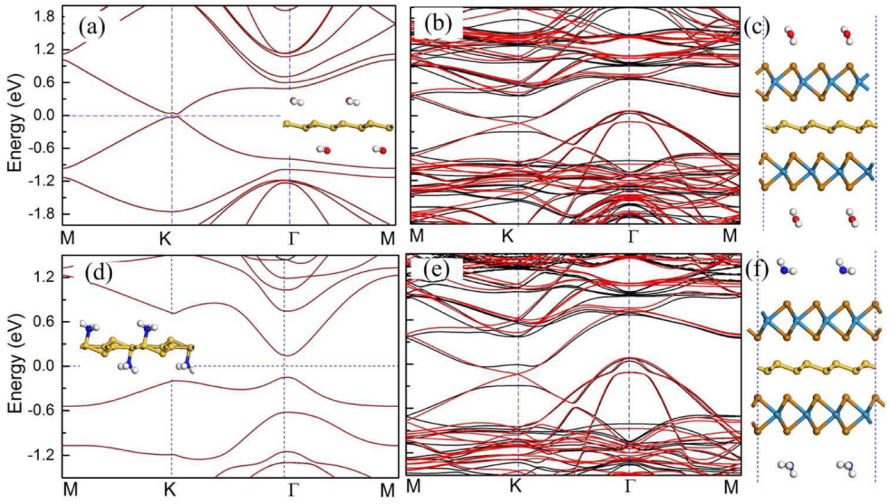

Figure 5. Protection of silicene against environmental degradation effects by the encapsulation. Electronic band structures of silicene with (a) physisorbed H_2O and (d) chemisorbed NH_3 exhibit significantly altered electronic and topological properties; the gas-adsorbed silicene structures are shown in the insets. In contrast, the properties of the QWs are largely unaffected by the adsorption of (b) H_2O and (e) NH_3; the gas-adsorbed QW structures are shown in (c) and (f). The electronic structures with (black lines) and without (red lines) the SOC are plotted in all cases, but they are indistinguishable in gas-adsorbed silicene in (a) and (d), indicating the non-TI nature of the structures.

DOI: 10.1021/acsami.5b05063
ACS Appl. Mater. Interfaces 2015, 7, 19226–19233

TI. The band states of the adsorbed gas molecules are located at a deep energy level around −2 eV, which have negligible effects on the properties of silicene. For other small molecules or chemical species, like H or OH, they can also significantly change the electronic properties of silicene and destroy its essential features (see SI Figure S6), and the encapsulation is expected to protect silicene against the environment degradation. We therefore conclude that the cladding layers WTe_2 enhance the SOC and enlarge the nontrivial band gap of silicene, and they also very effectively protect the silicene from environmental degradation effects.

DISCUSSION

The above results show that WTe_2 is an excellent cladding layer material that serves a dual purpose of enhancing the SOC in silicene via proximity effect and protecting silicene from the environmental gases. It should be noted, however, that there are other choices. Another TMDC, $MoTe_2$, also generates a substantial nontrivial band gap in encapsulated silicene: 137 meV for the AB stacking and 25.4 meV for the AA stacking (see Figure S3 in Supporting Information). We expect that suitable cladding materials may also include other TMDCs, such as WSe_2, $MoSe_2$, or even MoS_2. Furthermore, the same QW architecture design and the underlying working principles should also apply to encapsulated germanene, the graphene analogue of germanium, which has been predicted to exhibit QSH effect.[7] These possibilities may result in a new family of robust 2D TIs.

It is crucial that both sides of silicene be covered by the TMDC layers to avoid degradation of its properties in the air. The widely used wet transfer technique[43] is inadequate here; even Al_2O_3-capped silicene degrades readily once the Ag cover is removed during transfer because of the exposed bottom surface. The silicene encapsulated delamination technique,[8] where both the bottom and top surfaces are protected, provides a feasible way to fabricate the proposed TMDC/silicene/TMDC QW structure. It was recently reported that silicene can be directly grown on the surface of MoS_2,[44] and it is expected that the silicene/WTe_2 heterostructure also can be achieved using a similar experimental approach. Si was deposited on top of a cleaved TMDC layer from a thermally heated and ultrahigh vacuum crucible, and the subsequently transferred TMDC cladding layer[8] can be used to cover the synthesized silicene/WTe_2, forming the proposed QW structure.

In the present work we have used a unit-cell model to construct the QW structure due to computational constraints, and it introduces substantial intralayer strains in the silicene and TMDC layers. Such large lattice distortions are unsustainable by the weak interlayer vdW interactions; consequently, a more realistic QW structure is expected to undergo an intralayer relaxation to release the strain energy, resulting in stacking disorder and moiré patterns.[45] This strain release would make electronic structures dominated by the intralayer interactions closer to that of free-standing layers. In particular, the strain-induced upshift of the valence band around the Γ point (see Figure 1 and Figure 2) would be reduced significantly, restoring a sizable global band gap as in free-standing silicene. On the other hand, the opening of a large nontrivial band gap at the K point is expected to remain largely unaffected since this gap stems from the proximity SOC effect driven by the interlayer interaction, which has little dependence on the intralayer strain state. In experimentally synthesized QW structures, the most likely stacking pattern would be MA, which is a compromise between the intralayer strain release and interlayer binding energy gain.[45] Our calculations have shown (see Figure 2) that the QW in an MA stacking pattern possesses a large nontrivial band gap above 100 meV, making it suitable for room-temperature applications. This result is driven by the strong interlayer proximity SOC effect, which is expected to be present in other MA-stacked QWs. To support this conclusion, we have checked a series of encapsulated silicene in MA stacking with different degrees of interlayer misalignment, and the obtained nontrivial band gaps are all on the order of 100 meV with the energetically more favorable structures possessing larger gaps around 200 meV (see Figures S4 and S5 in Supporting Information). These results demonstrate that large nontrivial band gap in encapsulated silicene is a general phenomenon, which calls for experimental verification and further exploration for innovative device applications.

The tunability of the electronic properties of the topological phase is important for its applications in spintronic and FET devices. We examined the influence of a vertical applied electric field, and the results indicate that the nontrivial gap at the K point decreases almost linearly with increasing field, and it closes completely at 0.04 V/Å (see Figure S7). This controllability by a modest electric field is highly desirable for nanodevice applications.

CONCLUSION

Extensive first-principles calculations show that a hybrid QW structure with a monolayer silicene sandwiched between two TMDC layers forms a novel 2D TI with a drastically enhanced nontrivial band gap that is 2 orders of magnitude higher than its value in free-standing silicene. This underlying mechanism is from the strong SOC in the MTe_2 layers via the proximity effect, which is sensitive to the interlayer coupling and highly effective in generating QSH states with a large nontrivial band gap in silicene in the QW architecture. The cladding MTe_2 layers also protect silicene from the degradation effects by the environmental gases. The topological nature of the QW structure is explicitly demonstrated by the presence of metallic edge states that are characteristic of the QSH states in 2D TIs. We further show that the QSH states in encapsulated silicene are robust against stacking misalignments that will likely exist in synthesized QW structures due to the lattice mismatch between the silicene layer and the cladding MTe_2 layers. The present work offers a new design concept for a novel class of 2D TIs that can operate in room temperature environments, and our current results are expected to stimulate considerable interest and further exploration that could lead to innovative nanoscale device applications with the new TMDCs encapsulated silicene QW structure as a central component.

METHODS

Electronic Structure Calculations. First-principles calculations based on the density functional theory (DFT) were carried out using the Vienna ab initio simulation package (VASP).[46] The exchange correlation interaction was treated within the generalized gradient approximation (GGA-PBE).[47] The QW is periodic in the *xy* plane and separated by at least 10 Å along the *z* direction to avoid self-interactions. All the atoms in the unit cell are fully relaxed until the force on each atom is less than 0.01 eV/Å. The Brillouin zone integration was sampled by a 10 × 10 × 1 *k*-grid mesh. An energy cutoff of 400 eV was chosen for the plane wave basis. The SOC was included. To describe the vdW interaction, a semiempirical correction by the Grimme method[46] was adopted.

DOI: 10.1021/acsami.5b05063
ACS Appl. Mater. Interfaces 2015, 7, 19226−19233

Gas Adsorption. For the gas adsorption on free-standing silicene and QWs, 2 × 2 supercells for both structures were used, with a size of 7.3 Å × 7.3 Å. To reserve the structural symmetry and simulate the true situation when placing silicene or QWs in the ambient environments, the gas molecules, H_2O and NH_3, are placed on both sides of the structure. All structures are fully relaxed to obtain the binding energies and electronic properties.

■ ASSOCIATED CONTENT

Supporting Information

The Supporting Information is available free of charge on the ACS Publications website at DOI: 10.1021/acsami.5b05063.

Band structures of $MoTe_2$/Silicene/$MoTe_2$; structural model of the AB stacked $MoTe_2$/Silicene/$MoTe_2$ nanoribbon; band gap variation of the AA and random stacked QWs; electronic properties for five kinds of random stacked QWs; band structures of the H- and OH-terminated silicene, as well as the modulation of the electronic properties of the QW by a vertical electric field (PDF)

■ AUTHOR INFORMATION

Corresponding Authors

*E-mail: kouliangzhi@gmail.com.
*E-mail: sean.smith@unsw.edu.au.

Notes

The authors declare no competing financial interest.

■ ACKNOWLEDGMENTS

We would like to acknowledge the computational time provided by NCI (LE120100181-Enhanced merit-based access and support at the new NCI petascale supercomputing facility (2012-2015)). L.K. and X.T acknowledge financial support of UNSW Australias SPF01 project 6301 (CI Smith). C.F.C. was partially supported by the DOE through the Cooperative Agreement DE-NA0001982.

■ REFERENCES

(1) Qi, X.-L.; Zhang, S.-C. The Quantum Spin Hall Effect and Topological Insulators. *Phys. Today* **2010**, *63*, 33.

(2) Chang, Z.-Z.; Zhang, J.; Feng, X.; Shen, J.; Zhang, Z.; Guo, M.; Li, K.; Ou, Y.; Wei, P.; Wang, L.-L.; Ji, Z.-Q.; Feng, Y.; Ji, S.; Chen, X.; Jia, J.; Dai, X.; Fang, Z.; Zhang, S.-C.; He, K.; Wang, Y.; Lu, L.; Ma, X.-C.; Xue, Q.-K. Experimental Observation of the Quantum Anomalous Hall Effect in a Magnetic Topological Insulator. *Science* **2013**, *340*, 167−170.

(3) Hsieh, D.; Xia, Y.; Qian, D.; Wray, L.; Dil, J. H.; Meier, F.; Osterwalder, J.; Patthey, L.; Checkelsky, J. G.; Ong, N. P.; Fedorov, A. V.; Lin, H.; Bansil, A.; Grauer, D.; Hor, Y. S.; Cava, R. J.; Hasan, M. Z. A Tunable Topological Insulator in the Spin Helical Dirac Transport Regime. *Nature* **2009**, *460*, 1101−1105.

(4) Zhang, H.; Liu, C.-X.; Qi, X.-L.; Dai, X.; Fang, Z.; Zhang, S.-C. Topological Insulators in Bi_2Se_3, Bi_2Te_3 and Sb_2Te_3 with a Single Dirac Cone on the Surface. *Nat. Phys.* **2009**, *5*, 438−442.

(5) Vogt, P.; de Padova, P.; Quaresima, C.; Avila, J.; Frantzeskakis, E.; Asensio, M. C.; Resta, A.; Ealet, B.; le Lay, G. Silicene: Compelling Experimental Evidence for Graphene like Two-Dimensional Silicon. *Phys. Rev. Lett.* **2012**, *108*, 155501.

(6) Feng, B.; Ding, Z.; Meng, S.; Yao, Y.; He, X.; Cheng, P.; Chen, L.; Wu, K. Evidence of Silicene in Honeycomb Structures of Silicon on Ag (111). *Nano Lett.* **2012**, *12*, 3507−3511.

(7) Liu, C. C.; Feng, W.; Yao, Y. Quantum Spin Hall Effect in Silicene and Two-Dimensional Germanium. *Phys. Rev. Lett.* **2011**, *107*, 076802.

(8) Tao, L.; Cinquanta, E.; Chiappe, D.; Grazianetti, C.; Fanciulli, M.; Dubey, M.; Molle, A.; Akinwande, D. Silicene Field-effect Transistors Operating at Room Temperature. *Nat. Nanotechnol.* **2015**, *10*, 227−231.

(9) Wang, R.; Pi, X.; Ni, Z.; Liu, Y.; Lin, S.; Xu, M.; Yang, D. Silicene Oxides: Formation, Structures and Electronic Properties. *Sci. Rep.* **2013**, *3*, 3507.

(10) Feng, J.-W.; Liu, Y.-J.; Wang, H.-X.; Zhao, J.-X.; Cai, Q.-H.; Wang, X.-Z. Gas Adsorption on Silicene: A Theoretical Study. *Comput. Mater. Sci.* **2014**, *87*, 218−226.

(11) Qi, X.-L.; Zhang, S.-C. Topological Insulators and Superconductors. *Rev. Mod. Phys.* **2011**, *83*, 1057−1110.

(12) Hasan, M. Z.; Kane, C. L. Topological Insulator. *Rev. Mod. Phys.* **2010**, *82*, 3045−3067.

(13) Bernevig, B. A.; Hughes, T. L.; Zhang, S.-C. Quantum Spin Hall Effect and Topological Phase Transition in HgTe Quantum Wells. *Science* **2006**, *314*, 1757−1761.

(14) Yan, B.; Jansen, M.; Felser, C. A Large-Energy-Gap Oxide Topological Insulator Based on the Superconductor BaBiO3. *Nat. Phys.* **2013**, *9*, 709−711.

(15) Weng, H. M.; Dai, X.; Fang, Z. Transition-metal Pentatelluride ZrTe5 and HfTe5: a Paradigm for Large-gap Quantum Spin Hall Insulators. *Phys. Rev. X* **2014**, *4*, 011002.

(16) Ma, Y.; Dai, Y.; Kou, L.; Frauenheim, T.; Heine, T. Robust Two-Dimensional Topological Insulators in Methyl-Functionalized Bismuth, Antimony and Lead Bilayer Films. *Nano Lett.* **2015**, *15*, 1083−1089.

(17) Xu, Y.; Yan, B.; Zhang, H.-J.; Wang, J.; Xu, G.; Tang, P.; Duan, W.-H.; Zhang, S.-C. Large-Gap Quantum Spin Hall Insulators in Tin Films. *Phys. Rev. Lett.* **2013**, *111*, 136804.

(18) Song, Z. G.; Liu, C. C.; Yang, J. B.; Han, J. Z.; Fu, B. T.; Ye, M.; Yang, Y. C.; Niu, Q.; Lu, J.; Yao, Y. G. Quantum Spin Hall Insulators and Quantum Valley Hall Insulators of BiX/SbX (X = H, F, Cl and Br) Monolayers with a Record Bulk Band Gap. *NPG Asia Mater.* **2014**, *6*, 147.

(19) Guo, Z.-X.; Furuya, S.; Iwata, J.-I.; Oshiyama, A. Absence and Presence of Dirac Electrons in Silicene on Substrates. *Phys. Rev. B: Condens. Matter Mater. Phys.* **2013**, *87*, 235435.

(20) Suryanarayana, D.; Hsiao, R.; Gall, T. P.; Mccreary, J. M. Enhancement of Flip-Chip Fatigue Life by Encapsulation. *IEEE Trans. Compon., Hybrids, Manuf. Technol.* **1991**, *14*, 218.

(21) Scalise, E.; Houssa, M.; Cinquanta, E.; Grazianetti, C.; van den Broek, B.; Pourtois, G.; Stesmans, A.; Fanciulli, M.; Molle, A. Engineering the Electronic Properties of Silicene by Tuning the Composition of MoX_2 and GaX (X = S,Se,Te) Chalchogenide Templates. *2D Mater.* **2014**, *1*, 011010.

(22) Ding, Y.; Wang, Y. Electronic Structures of Reconstructed Zigzag Silicene Nanoribbons. *Appl. Phys. Lett.* **2014**, *104*, 083111.

(23) Kou, L.; Yan, B.; Hu, F.; Wu, S.-C.; Wehling, T. O.; Felser, C.; Chen, C.; Frauenheim, T. Graphene-Based Topological Insulator with an Intrinsic Bulk Gap above Room Temperature. *Nano Lett.* **2013**, *13*, 6251−6255.

(24) Kou, L.; Wu, S. C.; Felser, C.; Frauenheim, T.; Chen, C.; Yan, B. Robust 2D Topological Insulators in van der Waals Heterostructures. *ACS Nano* **2014**, *8*, 10448−10454.

(25) Xu, G.; Wang, J.; Yan, B.; Qi, X.-L. Topological Superconductivity at the Edge of Transition Metal Dichalcogenides. *Phys. Rev. B: Condens. Matter Mater. Phys.* **2014**, *90*, 10505.

(26) Chu, R.-L.; Liu, G.-B.; Yao, W.; Xu, X.; Xiao, D.; Zhang, C. Spin-Orbit-Coupled Quantum Wires and Majorana Fermions on Zigzag Edges of Monolayer Transition-Metal Dichalcogenides. *Phys. Rev. B: Condens. Matter Mater. Phys.* **2014**, *89*, 155317.

(27) Wang, Q. H.; Kalantar-Zadeh, K.; Kis, A.; Coleman, J. N.; Strano, M. S. Electronics and Optoelectronics of Two-dimensional Transition Metal Dichalcogenides. *Nat. Nanotechnol.* **2012**, *7*, 699−712.

(28) Cunningham, G.; Lotya, M.; Cucinotta, C. S.; Sanvito, S.; Bergin, S. D.; Menzel, R.; Shaffer, M. S. P.; Coleman, J. N. Solvent Exfoliation of Transition Metal Dichalcogenides: Dispersibility of

DOI: 10.1021/acsami.5b05063
ACS Appl. Mater. Interfaces 2015, 7, 19226−19233

Exfoliated Nanosheets Varies Only Weakly between Compounds. *ACS Nano* **2012**, *6*, 3468−3480.
(29) Zhu, Z. Y.; Cheng, Y. C.; Schwingenschloegl, U. Giant Spin-orbit-induced Spin Splitting in Two-dimensional Transition-metal Dichalcogenide Semiconductors. *Phys. Rev. B: Condens. Matter Mater. Phys.* **2011**, *84*, 153402.
(30) Zeng, H.; Dai, J.; Yao, W.; Xiao, D.; Cui, X. Valley Polarization in MoS2Monolayers by Optical Pumping. *Nat. Nanotechnol.* **2012**, *7*, 490−493.
(31) Amin, B.; Kaloni, T. P.; Schwingenschloegl, U. Strain Engineering of WS2, WSe2, and WTe2. *RSC Adv.* **2014**, *4*, 34561−34565.
(32) Kang, J.; Tongay, S.; Zhou, J.; Li, J.; Wu, J. Band Offsets and Heterostructures of Two Dimensional Semiconductors. *Appl. Phys. Lett.* **2013**, *102*, 012111.
(33) Pei, Q.-X.; Sha, Z.-D.; Zhang, Y.-Y.; Zhang, Y.-W. Effects of Temperature and Strain Rate on the Mechanical Properties of Silicene. *J. Appl. Phys.* **2014**, *115*, 023519.
(34) Castellanos-Gomez, A.; Poot, M.; Steele, G. A.; van der Zant, H. S. J.; Agraït, N.; Rubio-Bollinger, G. Elastic Properties of Freely Suspended MoS_2 Nanosheets. *Adv. Mater.* **2012**, *24*, 772−775.
(35) Qiao, Z.; Ren, W.; Chen, H.; Bellaiche, L.; Zhang, Z.; MacDonald, A. H.; Niu, Q. Quantum Anomalous Hall Effect in Graphene Proximity Coupled to an Antiferromagnetic Insulator. *Phys. Rev. Lett.* **2014**, *112*, 116404.
(36) Avsar, A.; Tan, J. Y.; Taychatanapat, T.; Balakrishnan, J.; Koon, G. K. W.; Yeo, Y.; Lahiri, J.; Carvalho, A.; Rodin, A. S.; O'Farrell, E. C. T.; Eda, G.; Castro Neto, A. H.; Özyilmaz, B. Spin-orbit Proximity Effect in Graphene. *Nat. Commun.* **2014**, *5*, 4875.
(37) Weeks, C.; Hu, J.; Alicea, J.; Franz, M.; Wu, R. Engineering a Robust Quantum Spin Hall State in Graphene via Adatom Deposition. *Phys. Rev. X* **2011**, *1*, 021001.
(38) Fu, L.; Kane, C. L. Topological Insulators with Inversion Symmetry. *Phys. Rev. B: Condens. Matter Mater. Phys.* **2007**, *76*, 045302.
(39) Fu, L.; Kane, C. L.; Mele, E. J. Topological Insulators in Three Dimensions. *Phys. Rev. Lett.* **2007**, *98*, 106803.
(40) Cinquanta, E.; Scalise, E.; Chiappe, D.; Grazianetti, C.; van den Broek, B.; Houssa, M.; Fanciulli, M.; Molle, A. Getting through the Nature of Silicene: an sp^2-sp^3 Two-dimensional Silicon Nanosheet. *J. Phys. Chem. C* **2013**, *117*, 16719−16724.
(41) Acun, A.; Poelsema, B.; Zandvliet, H. J. W.; van Gastel, R. The Instability of Silicene on Ag(111). *Appl. Phys. Lett.* **2013**, *103*, 263119. Molle, A.; Grazianetti, C.; Chiappe, D.; Cinquanta, E.; Cianci, E.; Tallarida, G.; Fanciulli, M. Hindering the Oxidation of Silicene with Non-reactive Encapsulation. *Adv. Funct. Mater.* **2013**, *23*, 4340−4344.
(42) Piner, R.; Li, H.; Kong, X.; Tao, L.; Kholmanov, I. N.; Ji, H.; Lee, W. H.; Suk, J. W.; Ye, J.; Hao, Y.; Chen, S.; Magnuson, C. W.; Ismach, A. F.; Akinwande, D.; Ruoff, R. S. Graphene Synthesis via Magnetic Inductive Heating of Copper Substrates. *ACS Nano* **2013**, *7*, 7495−7499.
(43) Chiappe, D.; Scalise, E.; Cinquanta, E.; Grazianetti, C.; van den Broek, B.; Fanciulli, M.; Houssa, M.; Molle, A. Two-Dimensional Si Nanosheets with Local Hexagonal Structure on a MoS_2 Surface. *Adv. Mater.* **2014**, *26*, 2096−2101.
(44) Sachs, B.; Wehling, T. O.; Katsnelson, M. I.; Lichtenstein, A. I. Adhesion and Electronic Structure of Graphene on Hexagonal Boron Nitride Substrates. *Phys. Rev. B: Condens. Matter Mater. Phys.* **2011**, *84*, 195414.
(45) Kresse, G.; Furthmueller, J. Efficient Iterative Schemes for Ab Initio Total-Energy Calculations Using a Plane-Wave Basis Set. *Phys. Rev. B: Condens. Matter Mater. Phys.* **1996**, *54*, 11169.
(46) Grimme, S. Semiempirical GGA-Type Density Functional Constructed with a Long-Range Dispersion Correction. *J. Comput. Chem.* **2006**, *27*, 1787−1799.
(47) Marzari, N.; Vanderbilt, D. Maximally Localized Generalized Wannier Functions for Composite Energy Bands. *Phys. Rev. B: Condens. Matter Mater. Phys.* **1997**, *56*, 12847.

DOI: 10.1021/acsami.5b05063
ACS Appl. Mater. Interfaces 2015, 7, 19226−19233